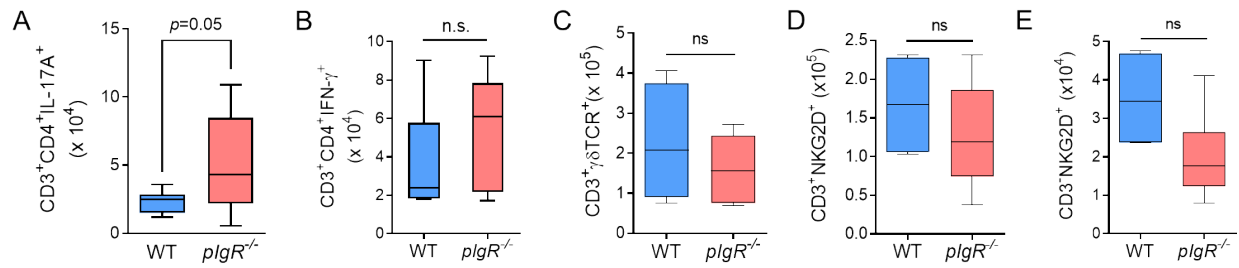
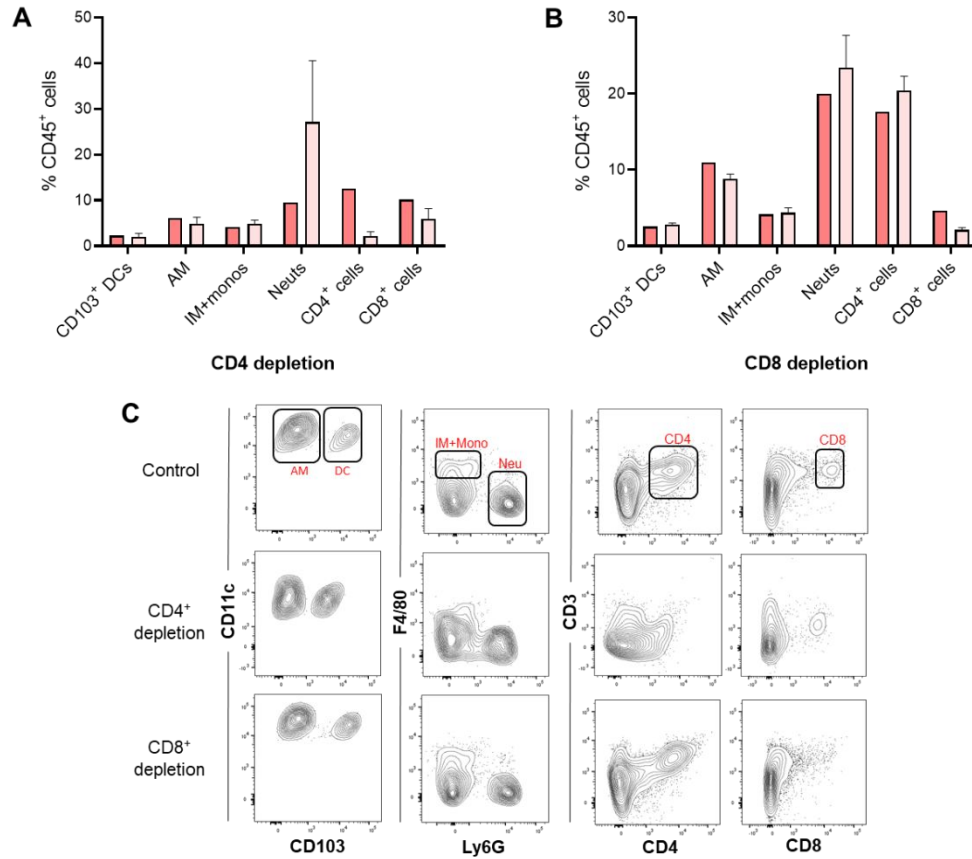


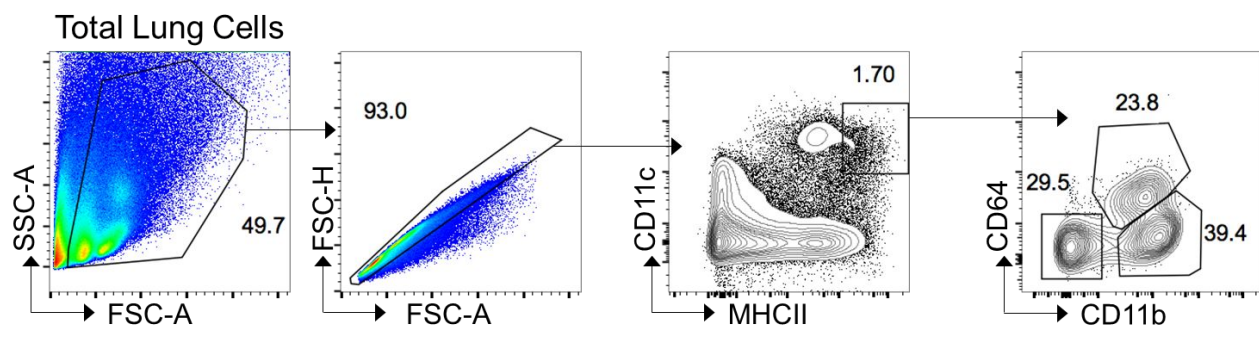
Supplemental Figures

Supplemental Figure 1. Quantification of IL-17A⁺ and IFN-γ⁺ CD4⁺ cells in the lungs of

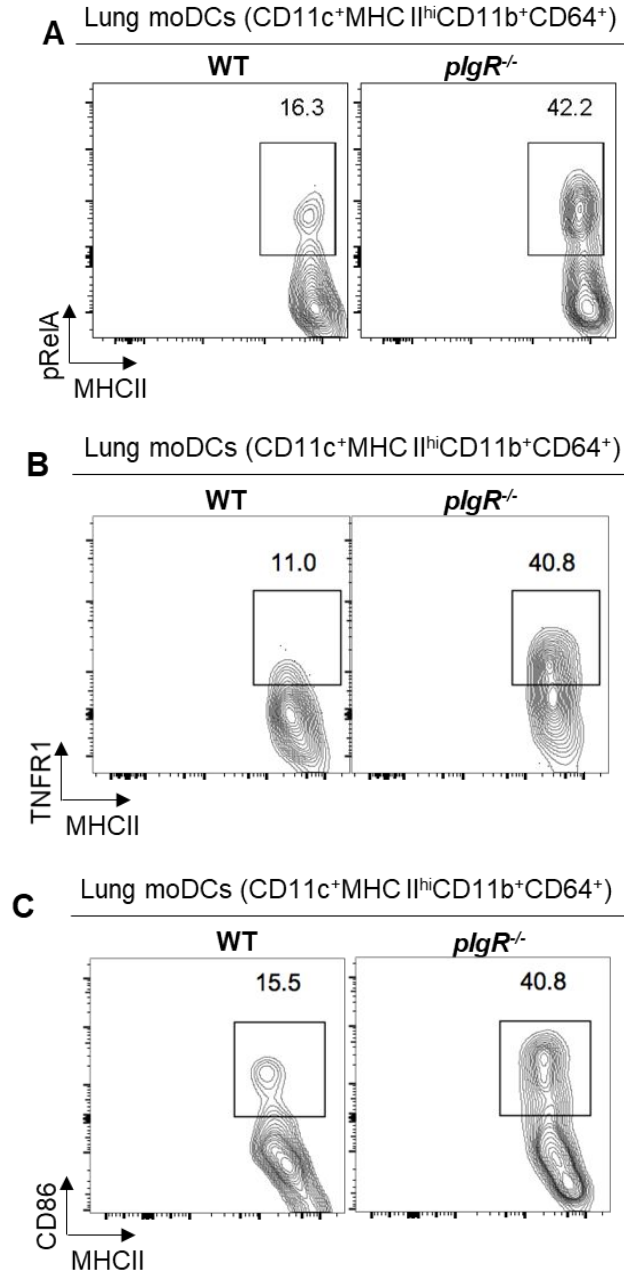
aged WT and *pIgR*^{-/-} mice. (A) Numbers of IL-17A⁺ CD4⁺ cells in lungs of 18-month-old WT and *pIgR*^{-/-} mice as determined by flow cytometry. (B) Numbers of IFN-γ⁺ CD4⁺ cells in lungs of 12-month-old WT and *pIgR*^{-/-} mice as determined by flow cytometry. (C-E) Numbers of γδ T cells (CD3⁺γδTCR⁺), NK-T cells (CD3⁺NKG2D⁺), and NK cells (CD3⁺NKG2D⁺) in lungs of 18-month-old WT and *pIgR*^{-/-} mice as determined by flow cytometry. n.s. = not significant, $p > 0.05$ by *t*-test.



Supplemental Figure 2. Effects of CD4 or CD8 depletion on other immune cell types in the lung. Red denotes *pIgR*^{-/-} control mice and pink denotes *pIgR*^{-/-} mice treated with CD4 or CD8-depleting antibodies. (A to B) % immune/inflammatory cells among CD45⁺ cells in the lungs of *pIgR*^{-/-} mice treated with CD4 or CD8-depleting antibodies for 1 month or no antibody. *n*=2-3 mice/group. (C) Gating strategy for A to B, including examples of flow cytometry plots in an untreated *pIgR*^{-/-} mouse (top row), a *pIgR*^{-/-} mouse treated with a CD8-depleting antibody for one month (middle row), and a *pIgR*^{-/-} mouse treated with a CD4 lymphocyte-depleting antibody for one month (bottom row). CD45⁺ cells were the parent population for all plots. AM=alveolar macrophages, DC=dendritic cells, IM=interstitial macrophages, Monos=monocytes, Neu=neutrophils.

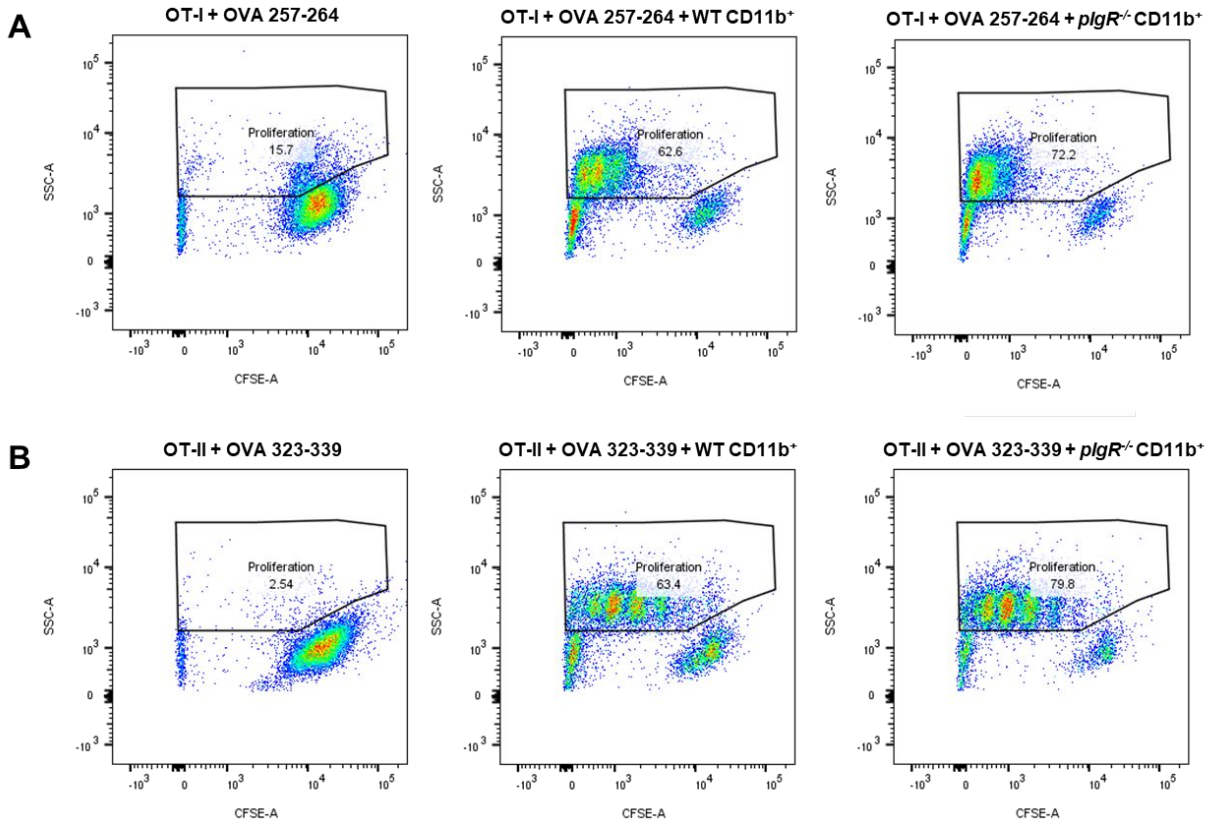


Supplemental Figure 3. Back-gating for moDC/cDC1/cDC2 flow cytometry plots. Gating strategy for identification of moDCs, cDC1, and cDC2 cells from total lung cells used in **Figure 4-6.**

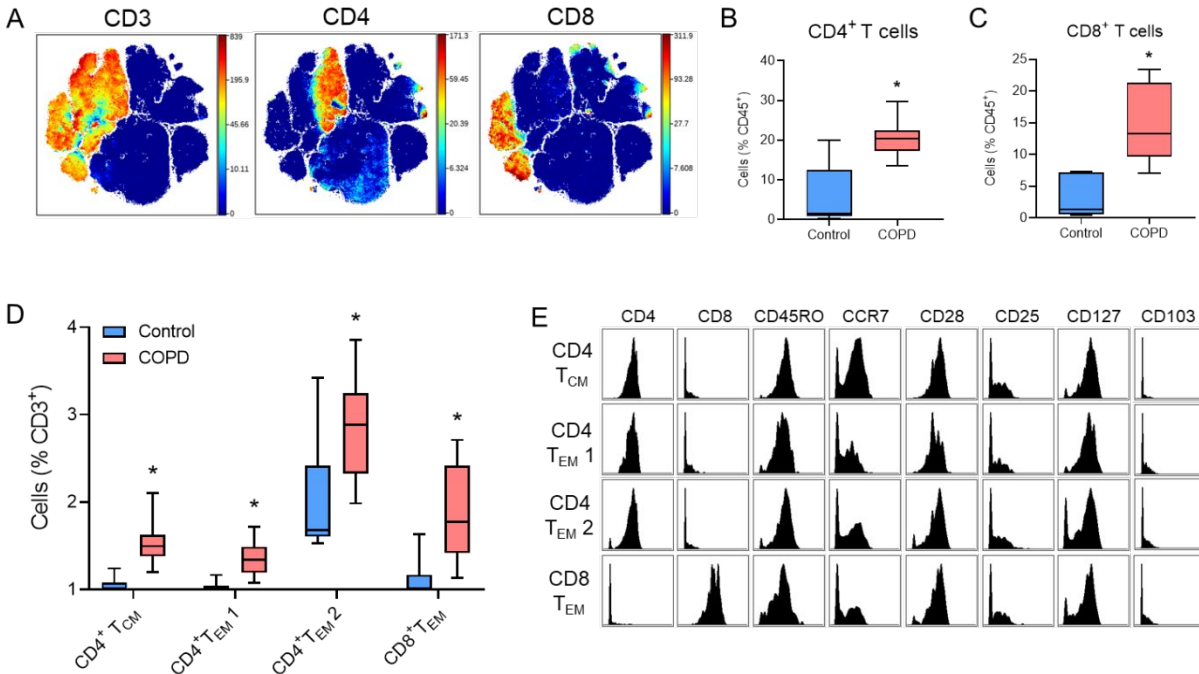


Supplemental Figure 4. Representative flow cytometry plots for moDC activation markers.

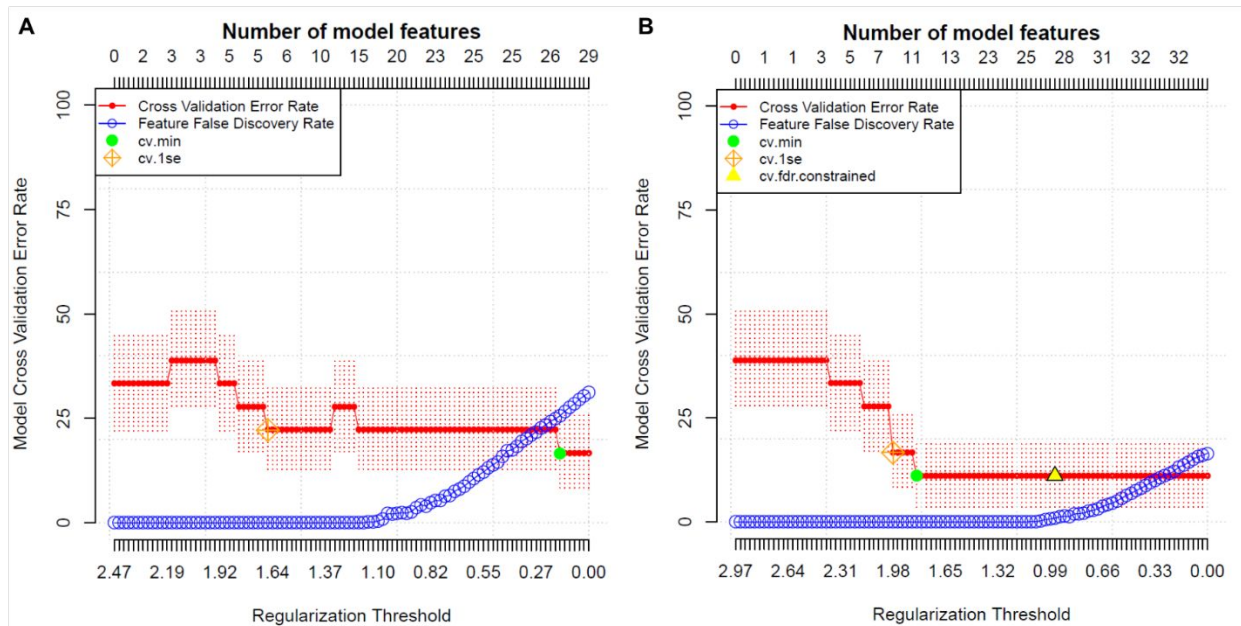
These flow cytometry plots correspond to data shown in **Figure 4C**. (A to C) Representative flow cytometry plots for pRelA⁺, TNFR1⁺, and CD86⁺ cells in 18-month-old WT and *pIgR*^{-/-} mice.



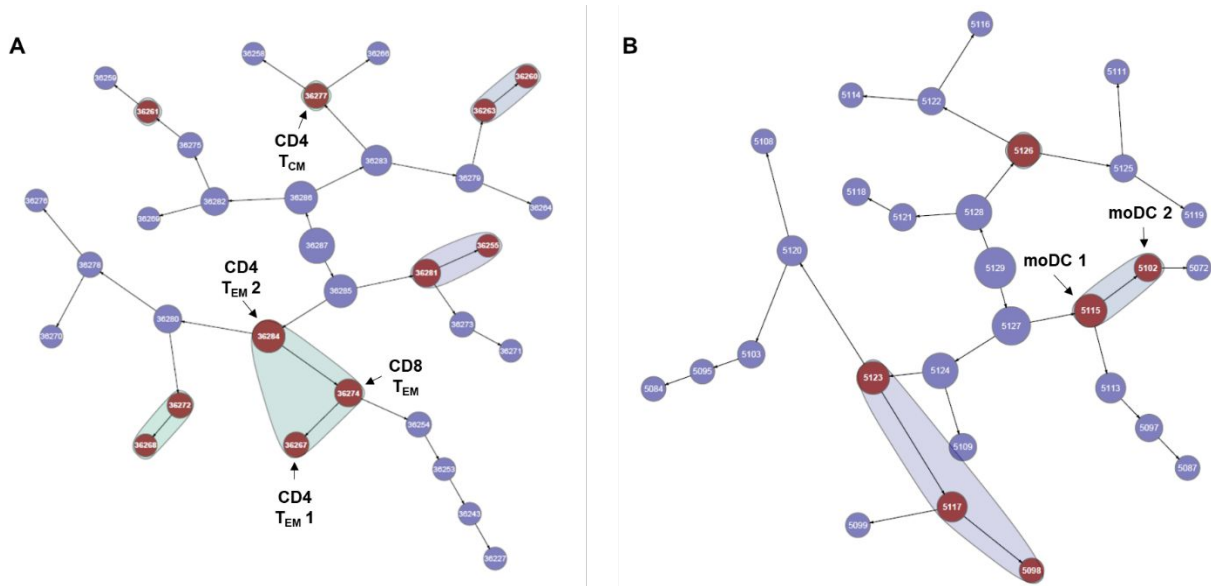
Supplemental Figure 5. Representative flow cytometry plots for mixed lymphocyte reaction experiments. These flow cytometry plots correspond to data shown in **Figure 4D and E.** **(A)** Representative flow cytometry plots showing OT-I proliferation by CFSE staining when cells were incubated in the presence of OVA 257-264 (left plot), OVA 257-264 and CD11b⁺ cells from 18-month-old WT mice (center panel), and OVA 257-264 and CD11b⁺ cells from 18-month-old *pIgR*^{-/-} mice. **(B)** Representative flow cytometry plots showing OT-II proliferation by CFSE staining when cells were incubated in the presence of OVA323-339 (left plot), OVA323-339 and CD11b⁺ cells from 18-month-old WT mice (center panel), and OVA323-339 and CD11b⁺ cells from 18-month-old *pIgR*^{-/-} mice.



Supplemental Figure 6. Increased effector memory CD4⁺ and CD8⁺ lymphocytes in the lungs of COPD patients. Single-cell suspensions were prepared from the lungs of 12 COPD patients and 6 controls without chronic respiratory disease and analyzed by mass cytometry. **(A)** Expression of CD3, CD4, and CD8 in viSNE clusters generated from live, single, CD45⁺ cells from all patients (total of 400,000 cells. **(B to C)**, Percentage of CD4⁺ and CD8⁺ cells among CD45⁺ cells in COPD and non-diseased control lungs. **(D)** Abundance (percentage of CD3⁺ cells) of the 4 lymphocyte clusters enriched in COPD lungs relative to controls. **(E)** Histograms of lymphocyte markers according to differentially abundant lymphocyte clusters as shown in **D**. **(B)**, * = $p < 0.001$ compared to control lungs (Mann-Whitney test); $n = 12$ COPD lungs and 6 control lungs. **(C)**, * = $p < 0.001$ compared to control lungs (t -test); $n = 12$ COPD lungs and 6 control lungs. **(D)** * = $p < 0.05$ compared to control lungs (Mann-Whitney test).



Supplemental Figure 7. Performance characteristics of Citrus models. These graphs correspond to the Citrus analyses described in **Figure 7-8**. The cross-validation error rate describes the ability of the Citrus model generated from all samples to describe behavior of a subset of samples. The cross-validation rate does not drop to zero because of unequal samples size between COPD and control samples. *cv.min* describes the model with the lowest cross-validation error rate and represents the minimum number of features needed to describe differential abundance in each cluster between COPD and control samples. *cv.1se* describes the model with the lowest cross-validation error rate within 1 standard error and also represents the minimum number of features needed to describe the differences between COPD and control samples. *cv.fdr.constrained* describes all of the different features below the false discovery rate (1%) and represents all the features required to describe differential abundance in each cluster between COPD and control samples.



Supplemental Figure 8. Citrus analyses for T lymphocyte and myeloid cell populations. In this visualization, each cluster generated by Citrus is depicted by a single node, with the size of the node indicating the proportional abundance of the cluster and red nodes indicating differentially abundant clusters between COPD and control lungs. **(A)** Citrus analysis showing cell clusters within the lymphocyte ($CD3^+$) viSNE islands. The labeled clusters were increased in COPD lungs. **(B)** Citrus analysis showing cell clusters within the myeloid cell ($CD11b^+CD11c^+HLA-DR^+$) viSNE island. The labeled clusters were increased in COPD lungs.

Supplemental Table 1. Demographic and clinical characteristics of patients evaluated in Figure 1.

	Lifelong non-smokers (n=8)	COPD (n=12)
Age – yr.		
Mean	61.9	56.7
Range	55-69	44-65
Sex – No. (%)		
Male	5 (62.5)	6 (50)
Female	3 (37.5)	6 (50)
Race/ethnicity No. (%)		
White non-Hispanic	-	11 (92.7)
Black	-	1 (8.3)
FEV1/FVC ratio		
Mean	92.5	27.2
Range	61-117	21-42
FEV1, % predicted		
Mean	101	20.9
Range	88-109	12-29
FVC, % predicted		
Mean	79	63
Range	74-84	37-93
Tobacco history (pack-years)		
Mean	-	38.8
Range	-	21-75
Alpha-1-antitrypsin deficiency		
No. (%)	-	0 (0)

Supplemental Table 2. Demographic and clinical characteristics of patients evaluated in Figure 7 and 8.

	Control (n=6)	COPD (n=12)
Age – yr.		
Mean	35.5	57.8
Range	14-61	46-66
Sex – No. (%)		
Male	1 (17)	6 (50)
Female	3 (50)	6 (50)
Unknown	2 (33)	0 (0)
Race/ethnicity		
White non-Hispanic	3 (50)	12 (100)
African American	2 (33)	0 (0)
Hispanic/Latino	1 (17)	0 (0)
FEV1/FVC ratio		
Mean	-	27.8
Range	-	21-34
FEV1, % predicted		
Mean	-	16.5
Range	-	10-25
FVC, % predicted		
Mean	-	46.1
Range	-	36-62
Tobacco history (pack-years)		
Mean	-	45.7
Range	0-30	10-90
Current smoker		
No. (%)	4 (66)	0 (0)
Alpha-1-antitrypsin deficiency		
No. (%)	-	3 (25)

Supplemental Table 3. List of flow cytometry antibodies.

Figure	Marker	Fluorophore	Clone
Fig. 2	CD45	FITC	30-F11
Fig. 2	CD3	AF 700	17A2
Fig. 2	CD8	BV 710	53-6.7
Fig. 2	CD4	BV 510	RM4-5
Fig. 2	CD19	BV 570	6D5
Fig. 2	CD11c	APC	N418
Fig. 2	CD103	PE	2E7
Fig. 2	F4/80	APC-Cy7	BM8
Fig. 2	Ly6G	PE-Cy7	IA8
Fig. 5, 6	CD3	APC/Cy7	145-2C11
Fig. 5, 6	CD4	PE/Cy7	GK1.5
Fig. 5, 6	CD8	APC	53-6.7
Fig. 4, 5, 6	CD11c	APC/Cy7	N418
Fig. 4, 5, 6	CD11b	PE/Cy7	M1/70
Fig. 4, 5, 6	MHCII	Brilliant violet 421	M5/114/15.2
Fig. 4, 5, 6	CD64	PerCP/Cy5.5	X54-5/7.1
Fig. 4, 5, 6	pRelA	APC	93H1
Fig. 4, 5, 6	TNFR1	PE	HM104
Fig. 4, 5, 6	CD86	APC/Cy7	GL-1
Fig. S1	Live/dead	Ghost UV 450	
Fig. S1	CD45	Alexa Fluor 700	30-F11
Fig. S1	CD3	BV786	145-2C11
Fig. S1	CD4	PE-Cy5	129.19
Fig. S1	IL-17A	PE-Cy7	eBio17B7

Supplemental Table 4. List of mass cytometry antibodies.

Figure	Marker	Metal conjugate
Fig. 7 and 8	CD45	89Y
Fig. 7 and 8	CD19	142Nd
Fig. 7 and 8	CD11b	144Nd
Fig. 7 and 8	CD4	145Nd
Fig. 7 and 8	CD8a	146Nd
Fig. 7 and 8	CD11c	147Sm
Fig. 7 and 8	CD16	148Nd
Fig. 7 and 8	CD127	149Sm
Fig. 7 and 8	CD86	150Nd
Fig. 7 and 8	HLA-DR	151Eu
Fig. 7 and 8	CD36	152Sm
Fig. 7 and 8	CCR4	153Eu
Fig. 7 and 8	CD163	154Sm
Fig. 7 and 8	CD169	158Gd
Fig. 7 and 8	FOXP3	159Tb
Fig. 7 and 8	CD14	160Gd
Fig. 7 and 8	CD103	161Dy
Fig. 7 and 8	CD28APC +anti-APC	162Dy
Fig. 7 and 8	CD34	163Dy
Fig. 7 and 8	CD45RO	164Dy
Fig. 7 and 8	CD64-PE + anti- PE	165Ho
Fig. 7 and 8	CD24	166Er
Fig. 7 and 8	CCR7	167Er
Fig. 7 and 8	CD206	168Er
Fig. 7 and 8	CD25	169Tm
Fig. 7 and 8	CD3	170Er
Fig. 7 and 8	CD68	171Yb
Fig. 7 and 8	CD38	172Yb
Fig. 7 and 8	CCR2 FITC+ anti-FITC	174Yb

Fig. 7 and 8	CD56	176Yb
Fig. 7 and 8	Nuc acid --Ir	191/193
Fig. 7 and 8	Cisplatin	198Pt